

UniPCB: A Unified Vision-Language Benchmark for Open-Ended PCB Quality Inspection

Fuxiang Sun^{13*}, Xi Jiang^{2*}, Jiansheng Wu³, Haigang Zhang^{1†}, Feng Zheng^{2†}, Jinfeng Yang¹

¹Shenzhen Polytechnic University ²Southern University of Science and Technology

³University of Science and Technology Liaoning

sunfuxiang@mail.szpu.edu.cn, jiangx2020@mail.sustech.edu.cn,

wujiansheng@ustl.edu.cn, jfyang@szpu.edu.cn,

zhanghg@szpu.edu.cn, f.zheng@ieee.org

Abstract

Multimodal Large Language Models (MLLMs) show promise for general industrial quality inspection, but fall short in complex scenarios, such as Printed Circuit Board (PCB) inspection. PCB inspection poses unique challenges due to densely packed components, complex wiring structures, and subtle defect patterns that require specialized domain expertise. However, a high-quality, unified vision–language benchmark for quantitatively evaluating MLLMs across PCB inspection tasks remains absent, stemming not only from limited data availability but also from fragmented datasets and inconsistent standardization. To fill this gap, we propose UniPCB, the first unified vision-language benchmark for open-ended PCB quality inspection. UniPCB is built via a systematic pipeline that curates and standardizes data from disparate sources across three annotated scenarios. Furthermore, we introduce PCB-GPT, an MLLM trained on a new instruction dataset generated by this pipeline, utilizing a novel progressive curriculum that mimics the learning process of human experts. Evaluations on the UniPCB benchmark show that while existing MLLMs falter on domain-specific tasks, PCB-GPT establishes a new baseline. Notably, it more than doubles the performance on fine-grained defect localization compared to the strongest competitors, with significant advantages in localization and analysis. We will release the instruction data, benchmark, and model to facilitate future research.

1 Introduction

In the field of electronic information engineering, PCBs are fundamental components that directly determine the performance and reliability of electronic products. Unlike conventional industrial anomaly detection (IAD) scenarios, PCB quality inspection poses more complex challenges due to its highly dense geometric layouts, repetitive patterns, and strict

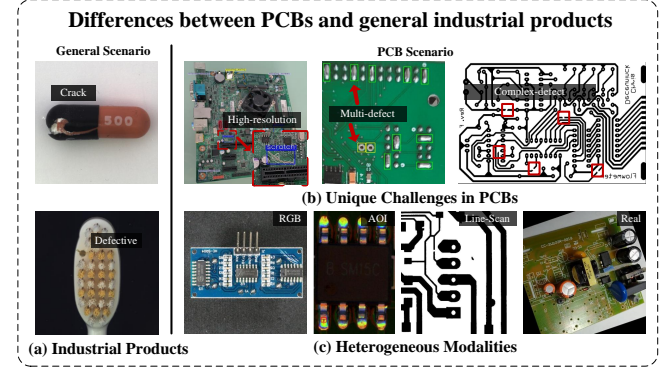


Figure 1: Comparison between general industrial products and PCB inspection. (a) General products with obvious surface defects. (b) Unique PCB challenges: dense patterns, defect co-occurrence, and subtle cues. (c) Diverse imaging modalities are required to capture different defect characteristics.

precision requirements. Moreover, defects on PCBs often appear as subtle, pixel-level variations, which can be easily obscured by background details and are highly prone to being confused with normal design structures such as traces and solder pads [Ling and Isa, 2023; Sankar *et al.*, 2022].

Although the image understanding capabilities of general-purpose MLLMs, such as Qwen-VL series [Wang *et al.*, 2024; Bai *et al.*, 2025; Yang *et al.*, 2025], InternVL series [Zhu *et al.*, 2025; Wang *et al.*, 2025], and LLaVA series [Li *et al.*, 2024a; Li *et al.*, 2024b], have steadily improved, their performance remains suboptimal when applied to highly specialized industrial scenarios like PCB quality inspection. Current general models lack the domain-specific knowledge required for PCB quality inspection, making it difficult for them to reliably distinguish normal circuit designs from genuine manufacturing defects. Similarly, pioneering IAD approaches such as AnomalyGPT [Gu *et al.*, 2024] are largely limited to coarse-grained classification and descriptive tasks, and struggle to handle the high complexity and fine-grained characteristics of PCB defects. Nevertheless, from a task-oriented perspective, MLLMs still have the potential to support the entire PCB quality inspection workflow. They can be applied to defect localization and identification, as well as subsequent analysis and risk assessment,

*Contributed Equally.

†Corresponding authors.

with interpretable reasoning to aid final decision-making.

The performance of MLLMs in domain-specific applications is fundamentally constrained by the quality and diversity of vision-language data. Although some prior work [Yu *et al.*, 2025a] attributes the reliance on a limited number of datasets, such as DeepPCB [Tang *et al.*, 2019], to the scarcity of publicly available resources, we argue that the primary obstacle is not merely the scarcity of data, but rather its systemic disarray, severe fragmentation, inconsistent quality, and a complete lack of unified standards. This fragmentation is evident as many datasets are narrow in scope, often confined to a single modality (e.g., RGB images) and limited defect classes. Consequently, they fail to capture the critical distributional shifts that occur as bare printed circuit board (BPCB) evolve into assembled printed circuit board (PCBA). Compounding this, a more fundamental problem—the absence of industry-wide definitions and annotation standards—renders fair comparison across fragmented datasets nearly impossible, leaving the field without a unified benchmark for the systematic and reliable evaluation of complex inspection models.

To systematically study these challenges, we introduce UniPCB, a large-scale, multi-scenario vision–language benchmark tailored for PCB quality inspection. Unlike existing datasets that focus on a single inspection task, UniPCB is built through a systematic data construction pipeline. Specifically, we curate publicly available PCB data from the Internet, covering multiple industrial imaging modalities, and collaborate with experienced engineers to rigorously define normal characteristics and defect criteria, thereby establishing a unified annotation protocol and consistent data split. Building on this foundation, we further bring multimodal instruction tuning methods [Zhang *et al.*, 2023; Ouyang *et al.*, 2022] into the PCB domain to construct conversation-style data for PCB inspection. UniPCB spans three inspection scenarios and 14 question types in a multi-turn, open-ended question-answer(QA) setting, comprising 6k images and 23k high-quality multimodal question–answer pairs.

Based on the UniPCB benchmark, we conduct a comprehensive evaluation of representative MLLMs [Comanici *et al.*, 2025; Bai *et al.*, 2025; Li *et al.*, 2024b; Wang *et al.*, 2025; Yu *et al.*, 2025b]. The results show that, due to limited domain knowledge, existing general-purpose MLLMs still suffer from noticeable hallucinations and inaccurate defect localization in PCB inspection. To mitigate these issues, we further propose PCB-GPT, a vision–language assistant for PCB quality inspection trained via a three-stage curriculum learning scheme. By mimicking the cognitive learning process of human experts, PCB-GPT effectively injects domain knowledge while improving the stability of structured outputs. As a result, PCB-GPT achieves advantages in multimodal dialogue, fine-grained defect identification, and overall inspection performance. Our contributions are summarized as follows:

- We propose a dedicated data construction and quality control pipeline for PCB inspection, enabling standardized processing of multi-source data, including cleaning, normalization, and dataset splitting.
- We construct UniPCB, to the best of our knowledge,

the first multimodal, multi-task benchmark designed for PCB quality inspection. UniPCB unifies two inspection levels, BPCB and PCBA, and covers three annotated scenarios and fourteen quality inspection subtasks.

- We introduce PCB-GPT, a vision–language assistant for PCB quality inspection trained with a three-stage curriculum learning strategy, which supports the full workflow from defect understanding to risk assessment.

2 Related Work

2.1 PCB Defect Analysis

As the backbone of electronic systems, the surface quality of PCB is critical to device reliability. Identifying anomalies, whether structural faults like open circuits or assembly errors like soldering defects, is therefore essential for yield optimization [Fonseca *et al.*, 2024; Anitha and Rao, 2017]. Although traditional automated systems (AOI, AXI) ensure inspection efficiency [Zhou *et al.*, 2023; Koblah *et al.*, 2023], their reliability often drops in scenarios involving occlusion or high component density. Deep learning methods, notably CNN, provide stronger feature extraction capabilities yet face significant hurdles in industrial adoption due to data scarcity and inconsistent annotations [Park *et al.*, 2023; Chen *et al.*, 2023]. To overcome these data-centric barriers and enable the rigorous evaluation of detection methods, we introduce UniPCB, a unified benchmark constructed from open-source PCB datasets.

2.2 MLLM

MLLMs typically bridge visual encoders with LLMs via cross-modal alignment to enable capabilities like captioning and visual question answering [Liu *et al.*, 2023]. This field has bifurcated into contrastive learning for retrieval (e.g., CLIP [Radford *et al.*, 2021]) and instruction-aligned generation (e.g., BLIP [Li *et al.*, 2022], LLaVA [Li *et al.*, 2024a]). While recent approaches have integrated region bounding boxes and open-vocabulary detection into instruction tuning to improve spatial grounding [Peng *et al.*, 2023; Minderer *et al.*, 2022], general-purpose MLLMs generally fail to satisfy the stringent requirements of complex industrial inspection, particularly regarding precise localization and specialized domain knowledge.

2.3 MLLM for Industrial Anomaly Detection

Bringing MLLMs into IAD has become a focal point of recent research [Yin *et al.*, 2024]. The field is pivoting from cascaded designs [Gu *et al.*, 2024; Li *et al.*, 2023]—which are prone to error accumulation—toward unified end-to-end frameworks. Notable approaches include Anomaly-R1 and OmniAD [Chao *et al.*, 2025; Zhao *et al.*, 2025a; Zeng *et al.*, 2025], which employ Group Relative Policy Optimization (GRPO) [Shao *et al.*, 2024] for improved reasoning, and VMAD [Deng *et al.*, 2025; Li *et al.*, 2025], which emphasizes fine-grained defect awareness. Meanwhile, domain-specific models like FabGPT [Jiang *et al.*, 2024b] expose the inadequacy of generalist MLLMs for intricate industrial tasks. However, advancement is stalled by the paucity of

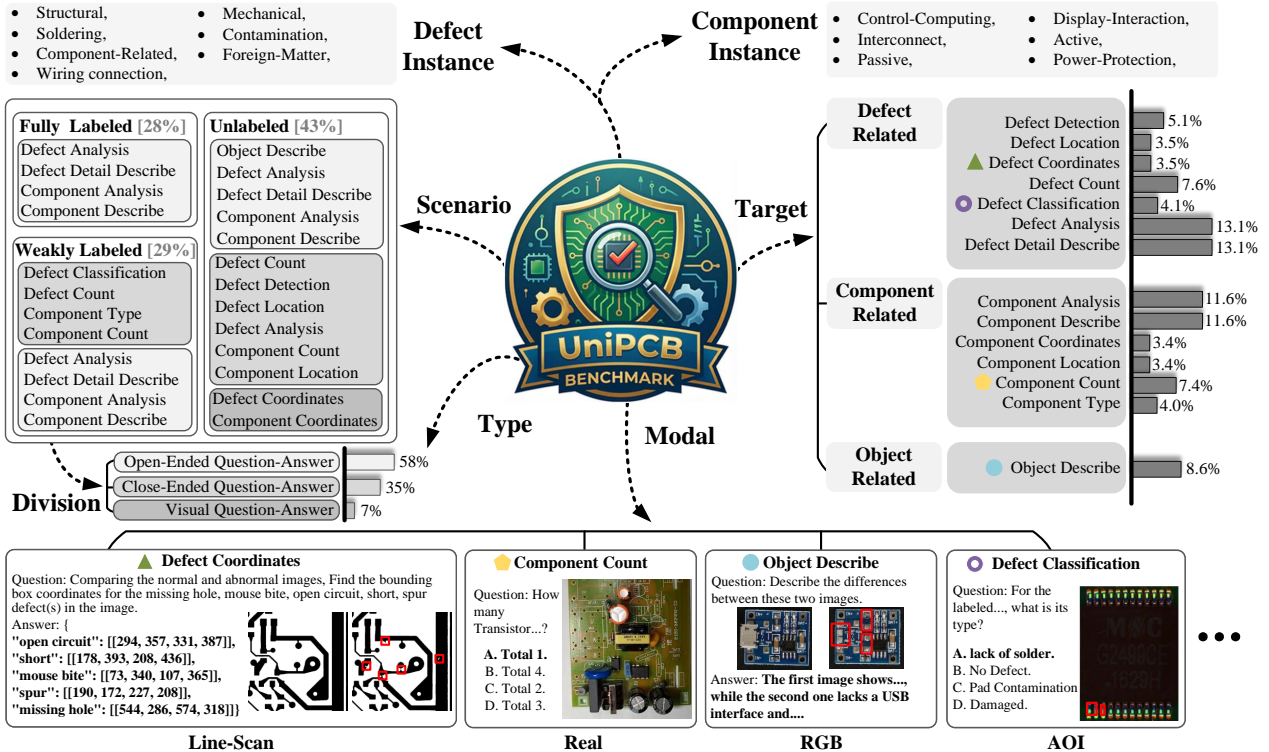


Figure 2: Overview of UniPCB Benchmark. We summarize the three annotation scenarios, unified defect and component taxonomies, task by target type, and the overall task proportions, with representative QA examples shown at the bottom.

high-quality instruction corpora and unified evaluation frameworks. Benchmarks such as MMAD [Jiang *et al.*, 2024a] and EIAD [Zhang *et al.*, 2025] reveal that mainstream models still lack the precision required for industrial deployment. Consequently, we investigate data curation and training strategies for PCB inspection to bridge these capability gaps.

3 UniPCB: Dataset and Benchmark

3.1 Challenges and Motivation

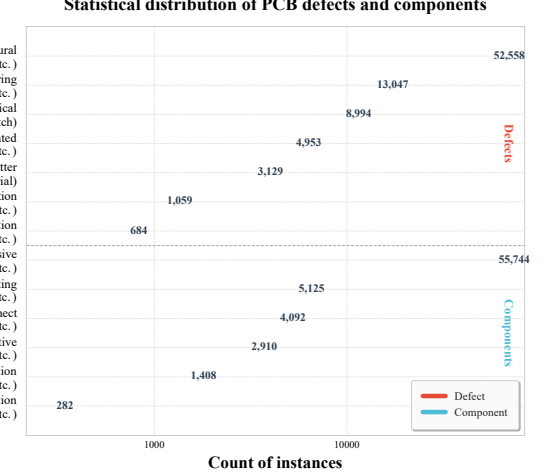
Unlike general industrial inspection targeting coarse textures, PCB quality inspection involves unique structural constraints (Fig. 1). Defects are often minute, and visually indistinguishable from normal circuit primitives (e.g., traces and pads), complicating detection. This challenge is compounded by heterogeneous imaging modalities, ranging from RGB to line-scan. To address this, we constructed a multi-source dataset using a strict cleaning pipeline. By implementing perceptual hashing deduplication, distortion filtering, and label standardization, we established a consistent benchmark for complex industrial scenarios.

Unified taxonomies To unify annotation information from different sources, we established a unified classification system for defects and components (Fig. 2). Defects are categorized into seven categories (e.g., structural, soldering, component-related, wiring connection, mechanical, contamination, foreign-matter), and components are organized into

Figure 3: Statistical distribution of defect and component instances under the unified taxonomy.

six functional domains (e.g., control-computing, interconnect, passive, active, display-interaction, power-protection). Fig. 3 summarizes the category-wise instance distribution under this taxonomy. All training data and benchmark annotations consistently adhere to these classification systems.

Task and knowledge construction Guided by practical inspection workflows, we defined 14 subtasks covering detec-



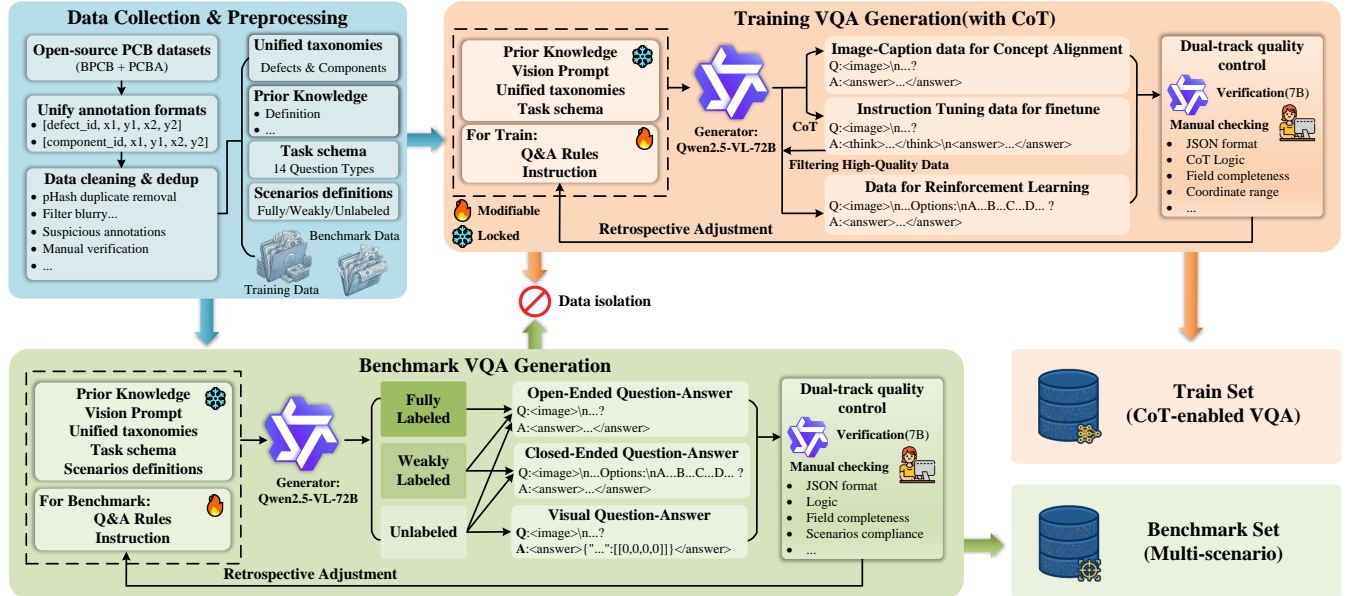


Figure 4: Data construction pipeline. We unify data sources, annotations, taxonomies, and a 14-type task schema, and construct two generation branches: a CoT-enabled training set and a multi-scenario benchmark. Each branch applies dual-track quality control with iterative prompt/rule refinement.

tion, counting, classification, localization, defect analysis, and reinspection recommendations. For each defect and component type, we created a knowledge base entry that includes a short definition, common causes, potential impact, and standardized phrasing. This structured knowledge supports the generation of diverse yet controlled questions and answers based on templates.

VQA data generation and quality control We developed a VQA generation pipeline using Qwen2.5-VL-72B-Instruct to transform annotated images into multi-turn QA pairs. We utilized adaptive templates to enforce standardized output formats, such as JSON coordinates for localization, across diverse modalities. To ensure data reliability, we implemented a dual-track quality control mechanism combining automated structural validation with hierarchical human review, where feedback is used to iteratively refine prompts for semantic and structural consistency.

3.2 The UniPCB Benchmark

Design Principles The UniPCB Benchmark aims to (i) simulate practical inspection workflows, encompassing 14 subtasks. (ii) require structured outputs wherever possible to enable automated and repeatable performance evaluation. (iii) deliberately include challenging cases such as small targets, severe occlusions, highly similar components, and multi-defect scenes.

Scenario definitions To evaluate the model’s robustness under different annotation schemes, we constructed three scenarios. In the fully labeled scenario, each query object is labeled with both category and bounding-box annotations to assess the model’s analytical capabilities with rich prior information. The weakly labeled scenario only provides

bounding-box annotations, requiring the model to infer categories and quantities from appearance and context. In the unlabeled scenario, no labels are provided. Instead, the prompt specifies the defect or component of interest, and the model must directly detect, localize, and describe it. To ensure fairness and comparability, the task instructions and template generation for the three scenarios are designed independently. Strict isolation and deduplication are applied throughout sample extraction and expansion. The overall data construction process is illustrated in Fig. 4.

Evaluation metrics The benchmark employs three complementary evaluation protocols. For open-ended question-answer (OQA), we utilize a powerful LLM as an evaluator. The average of these five scores is then calculated and normalized to the $[0,1]$ interval. In addition, we employ common natural language generation metrics such as BERTScore [Zhang *et al.*, 2019] and Sentence-BERT similarity [Reimers and Gurevych, 2019] as supplementary references. For closed-ended question-answer (CQA), including single-choice and multiple-choice questions, we calculate accuracy by matching predicted options against the correct answers, and when necessary, employ simple heuristics to extract option letters from free-form text. For visual question-answer (VQA), we match predicted boxes P and ground-truth boxes G using the Hungarian algorithm based on Intersection-over-Union (IoU) cost, considering a match valid if the IoU exceeds 0.3 for the same category. We then report Precision, Recall, and F1 scores. All subsequent experiments follow this unified protocol.

Statistic Analysis UniPCB features 6581 images and 23,359 bilingual QA pairs organized into three progressive scenarios. Notably, the task distribution moves beyond sim-

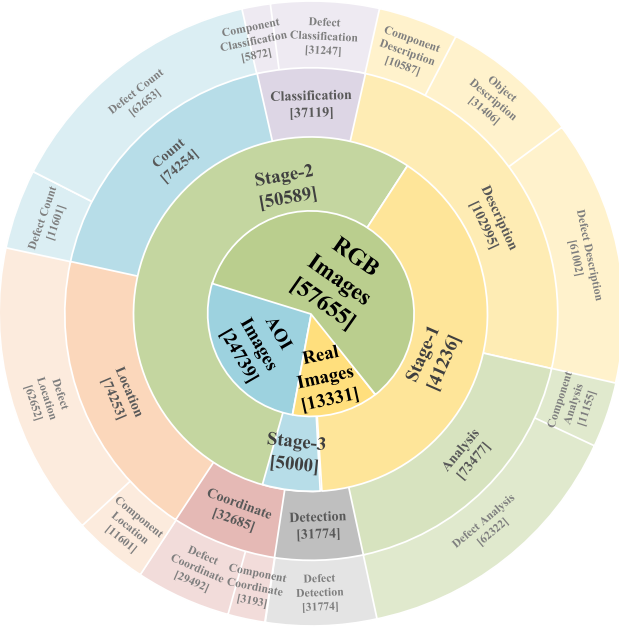


Figure 5: Rings from inner to outer represent imaging modalities (RGB/AOI/Real), data construction stages, and task families with fine-grained sample counts.

ple perception: a dominant portion of the benchmark is dedicated to Defect Analysis and Detail Description. This design compels models to transition from merely identifying where a defect is to reasoning why it occurred and what it implies, thereby evaluating the depth of industrial understanding rather than just surface-level detection.

3.3 Training Data

As illustrated in Fig. 5, the constructed dataset is stratified into three subsets spanning multiple imaging modalities, organized by training stages, task families, and fine-grained question types. The first stage comprises approximately 100k caption pairs from general and PCB domains, prioritizing high-quality samples to align visual features with standardized defect terminology. The second stage incorporates roughly 300k multi-turn dialogues under a unified schema, ensuring strict output formatting across diverse scenarios. The third stage uses a condensed set of approximately 5k verifiable samples (e.g., MCQ, JSON coordinates) to enable reward-based optimization. The detailed data split is provided in the Appendix.

4 PCB-GPT

General-purpose MLLMs often falter in PCB inspection due to the lack of domain-specific priors and the high demand for localization precision. To bridge this gap, we propose PCB-GPT. We introduce a curriculum learning strategy tailored to mimic the cognitive growth of a domain expert, progressively enhancing the model’s capabilities from basic recognition to complex reasoning.

4.1 Three-stage curriculum

Specifically, this strategy unfolds in three phases to endow PCB-GPT with: (i) PCB-specific visual semantics, (ii) instruction-following and structured generation, and (iii) verifiable decision-making ability via RL. We use Qwen2.5-VL-7B-Instruct as the base model and perform stage-wise optimization with LoRA [Hu *et al.*, 2022] while keeping the backbone frozen.

Stage-1: Concept Alignment We first align the visual encoder with PCB domain semantics using caption-style concept data. To preserve general visual understanding while injecting domain cues, we freeze the backbone and train LoRA only on the Query and Value projections of self-attention. This stage mainly improves the recognition of PCB components and defect concepts.

Stage-2: Instruction Tuning Next, we perform supervised instruction tuning on our multimodal QA data. We freeze the backbone and apply LoRA to all linear layers of the language model (excluding the output head). To encourage explicit reasoning and robust parsing, we supervise the model to generate responses in a unified structured format: `<think>...</think><answer>...</answer>`.

Stage-3: Reinforcement Learning with GRPO To further improve performance on verifiable tasks, we apply GRPO in Stage-3. For each prompt, the policy samples a group of candidate responses and receives rewards from automatic checkers. GRPO performs group-relative policy updates with a reference-regularized objective, and we additionally include a strict format bonus to stabilize structured outputs. In our implementation, we sample $n=8$ responses per prompt and apply KL regularization to the reference policy with coefficient 0.01.

Structured Reward for Verifiable Tasks Given an input sample x , the model generates an output y , from which we parse an answer segment $\hat{a}(y)$. For verifiable tasks with ground-truth g , we define:

$$R(x, y, g) = w_T \cdot \text{Acc}(\hat{a}(y), g) + w_F \cdot \mathbf{1}\{y \in \mathcal{F}\}, \quad (1)$$

where $\text{Acc}(\hat{a}(y), g) \in [0, 1]$ is the automatic correctness score (e.g., exact match for MCQ, and IoU-based matching F1 for BBOX), and $\mathbf{1}\{y \in \mathcal{F}\}$ equals 1 iff y strictly follows the structured output format defined in Stage-2, otherwise 0. We clip R to $[0, 1]$ and set $w_T = 0.9$, $w_F = 0.1$ in all experiments.

4.2 Implementation details

All stages were trained on eight NVIDIA A100-40GB GPUs. Stage 1-2 used Swift [Zhao *et al.*, 2025b] for supervised fine-tuning, while Stage 3 utilized Verl [Sheng *et al.*, 2025] for GRPO [Shao *et al.*, 2024] policy optimization. Inference and evaluation were conducted using vLLM [Kwon *et al.*, 2023].

5 Experiments

5.1 Overall Results on UniPCB Benchmark

Experimental setup We systematically evaluated a diverse array of multimodal models on the UniPCB benchmark, covering IAD MLLMs, open-source MLLMs, and commercial

Type	Model	Scale	Acc		S-BERT			BERTScore			F1	LLM as Judge	Average
			P2	P3	P1	P2	P3	P1	P2	P3			
Commercial MLLM	GPT5-Main	–	<u>73.1</u>	<u>66.1</u>	77.0	71.2	72.2	70.5	71.0	70.5	<u>20.2</u>	73.7	66.5
	Gemini2.5-Pro	–	76.4	68.5	<u>71.9</u>	<u>69.6</u>	<u>66.5</u>	<u>67.7</u>	<u>69.3</u>	<u>64.9</u>	23.6	<u>70.8</u>	<u>64.9</u>
	Gemini2.5-Flash	–	63.4	46.5	70.9	67.4	63.6	67.6	68.5	63.7	17.0	69.1	59.8
IAD MLLM	EMIT	8B	36.4	48.5	69.3	60.0	70.2	69.2	67.1	70.0	10.5	60.2	56.1
	IAD-R1	7B	58.9	50.1	56.9	54.7	56.4	61.3	60.0	60.5	15.2	36.0	51.0
	AnomalyGPT	7B	12.9	12.3	37.4	50.1	47.0	58.3	61.4	60.0	–	34.6	37.4
Open Source MLLM	DeepSeek2VL	16B	17.5	24.4	57.8	47.3	53.3	64.6	62.2	63.0	–	39.6	43.0
	InternVL2.5	8B	56.7	39.0	66.0	64.0	66.6	68.1	67.7	65.6	14.0	58.7	56.6
	InternVL3	8B	52.9	47.2	64.7	56.0	66.1	67.2	62.1	67.5	18.0	56.5	55.9
	InternVL3.5	8B	57.5	43.5	65.5	53.7	64.5	67.7	61.1	<u>68.0</u>	19.5	55.5	55.6
	LLaVA-OV	8B	61.6	<u>55.4</u>	<u>73.2</u>	56.7	<u>68.7</u>	<u>70.0</u>	67.1	67.9	–	59.8	58.1
	MiMo-V2-Flash	15B	40.0	47.7	42.0	64.0	45.4	57.8	67.0	61.4	16.1	42.6	48.4
	MiniCPM-V4.5	8B	53.9	54.0	57.7	<u>66.3</u>	65.6	61.0	67.9	67.2	15.5	58.2	56.7
	Qwen2.5-VL	7B	53.2	44.2	66.7	50.4	63.7	68.1	60.7	66.5	<u>22.3</u>	54.3	55.0
	Qwen3-VL-Instruct	8B	61.5	48.7	64.8	66.2	64.6	65.0	<u>68.2</u>	64.1	22.2	<u>61.0</u>	<u>58.6</u>
	Qwen3-VL-Think	8B	<u>65.6</u>	54.6	64.9	65.5	58.0	65.6	66.5	65.0	20.1	58.7	58.5
	PCB-GPT (Ours)	7B	72.5	66.4	73.4	69.0	67.1	70.1	70.0	67.4	51.1	65.8	67.3

Table 1: Quantitative comparison on the UniPCB Benchmark across Commercial, IAD, and Open-Source MLLMs. Bold and underlined values indicate the best and second-best performance within each model category, respectively. P1, P2, and P3 denote the fully labeled, weakly labeled, and unlabeled settings.

MLLMs. To ensure fair comparison, a unified prompt template and consistent decoding settings were employed across all evaluations. Furthermore, for unlabeled scenarios, we adopted a dual-image input strategy—pairing a normal reference with the query image to facilitate defect detection via comparison. Apart from this specific setting, all other tasks utilized single-image inputs.

Main results Table 1 presents the overall quantitative results on the UniPCB Benchmark. In general, commercial models maintain a competitive edge in semantic consistency and discriminative capabilities. GPT-5 retains the lead in open-ended QA, while Gemini 2.5 Pro achieves the highest accuracy in closed-ended QA, reflecting the robustness of commercial models in text comprehension and option discrimination. Among open-source models, PCB-GPT achieves the highest average score and demonstrates significant superiority in coordinate localization. This finding highlights that within PCB quality inspection scenarios, strong language generation and semantic alignment do not automatically translate into reliable spatial localization. It further reveals that mainstream MLLMs still have considerable room for improvement regarding fine-grained localization and structured output generation. In contrast, MLLMs designed for IAD maintain decent performance on semantic similarity metrics but generally exhibit weaker localization capabilities, leading to a notable gap in overall scores compared to general-purpose MLLMs. This aligns with the task assumptions of anomaly detection methods, which focuses on coarse-grained decisions about whether an anomaly exists

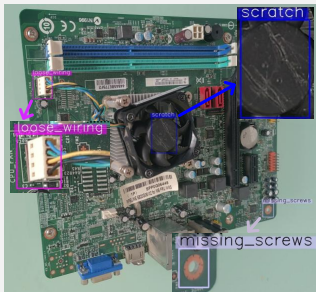
Model	0-shot				1-shot			
	Acc	Prec	Rec	F1	Acc	Prec	Rec	F1
GPT5-Main	65.1	39.9	28.2	33.0	48.3	35.6	85.7	50.3
AnomalyGPT	70.7	46.0	<u>44.6</u>	<u>45.3</u>	42.3	30.6	88.2	45.5
PCB-GPT (Ours)	63.8	40.6	72.1	52.1	77.8	50.6	76.0	61.0

Table 2: Evaluation results on the PCB-Bank dataset. We report Accuracy (Acc), Precision (Prec), Recall (Rec), and F1-score under 0-shot and 1-shot settings.

and roughly where it occurs. Our benchmark instead emphasizes fine-grained defect analysis and precise localization, exposing a pivotal gap in existing capabilities.

5.2 Cross-Dataset Generalization

We extended the evaluation to the external PCB-Bank dataset [Yao *et al.*, 2024] to verify cross-dataset generalization. As shown in Table 2, in the zero-shot setting, AnomalyGPT exhibits high accuracy but low recall. This reflects a bias toward the majority non-defect class due to data imbalance. PCB-GPT achieves a higher F1-score, indicating better sensitivity to actual defects. In the one-shot setting, competitor models show a sharp increase in recall paired with a drop in precision, implying an over-prediction of defects when provided with visual references. In contrast, PCB-GPT utilizes the in-context information to improve both accuracy and precision.



Question:
For the defect in the image, please analyze its root cause and provide suggestions.

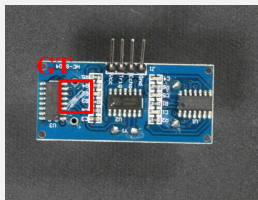
Answer:

<think>The loose wiring issue indicates potential damage to the circuitry due to improper connections or physical stress on the board. The scratch on the fan suggests mechanical damage that could compromise insulation or signal integrity. Missing screws imply structural instability which can lead to further issues like short circuits or component detachment.</think>

<answer>The loose wiring issue suggests potential damage to the circuitry caused by improper connections or physical stress on the board, which may result in intermittent connectivity problems or complete failure of the affected components. The scratch on the fan indicates mechanical damage that could compromise the insulation properties or signal integrity, potentially leading to short circuits or erratic behavior within the board's operation. Missing screws imply structural instability, which can cause components to become loose over time, increasing the risk of short circuits, open circuits, or even the detachment of critical parts from the board. Addressing these defects promptly through repair or replacement will ensure the reliability and longevity of the motherboard.</answer>

Question:

Comparing the normal and abnormal images, find the bounding box coordinates for the defect(s) in the image.



Answer:

<think>The area of concern is located on the left side of the PCB, specifically near the edge where the copper trace appears to have been scratched. The scratch is visible as a line that disrupts the continuity of the copper layer, indicating a potential defect. The bounding box should encapsulate this area precisely.</think>

<answer>{"scratch": [[313, 449, 438, 565]]}</answer>

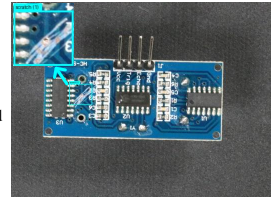


Figure 6: Qualitative examples of PCB-GPT on the UniPCB benchmark. Key logical evidence within the `<think>` block is highlighted in red, which explicitly guides the model to generate the final correct answers (highlighted in blue).

Model	CoT	Acc	F1	OQA Score	Average
Qwen2.5-VL	X	48.7	22.3	59.9	43.6
+BaseData	X	60.1	30.0	66.1	52.1
+Stage1	X	57.3	15.2	62.8	45.1
+Stage1,2	X	57.1	22.7	69.3	49.7
+Stage1,2,3	X	65.6	27.3	69.8	54.2
+Stage1,2	✓	63.3	38.9	67.0	56.4
+Stage1,2,3	✓	69.5	51.1	69.0	63.2

Table 3: Ablation on Qwen2.5-VL-7B. BaseData refers to unpartitioned and uncurated generated data.

5.3 Ablation Studies and Analysis

Phased training and data strategy ablations were conducted on Qwen2.5-VL-7B, with results detailed in Table 3. Even without phased training, incorporating raw base data yields stable gains, suggesting that broader domain coverage enhances general recognition and QA capabilities. However, improvements in localization metrics remain limited and suboptimal. This implies that precise localization depends more on subsequent instruction alignment and structured output constraints than on mere data accumulation. We further compared the contributions of different training stages. The concept alignment stage mainly improved semantic metrics but had limited impact on overall performance, indicating that supplementing PCB domain knowledge alone is insufficient for complex quality inspection. The introduction of instruction fine-tuning improved all metrics, demonstrating that instruction supervision effectively translates knowledge into task-oriented outputs. Incorporating reinforcement learning further enhanced performance, particularly in output consistency and verifiability. This confirms that reward signals derived from verifiability.

able samples help stabilize optimization for precisely evaluable tasks, thereby boosting robustness. Additionally, we examined the role of Chain-of-Thought (CoT) supervision. Models trained with CoT achieved superior scores, attributed not to increased text length but to the explicit 'reasoning before answering' constraint. This compels the model to better utilize existing information for decision-making, enhancing the reliability of structured outputs like coordinates. Conversely, models without CoT showed a slight advantage in open-ended QA, likely because omitting the reasoning process reduces redundancy, yielding more concise responses. However, this advantage is restricted to open-ended tasks and offers limited overall performance improvement.

5.4 Qualitative Analysis

Fig. 6 visualizes the inference process, where the CoT mechanism bridges visual perception and structured output. In the defect analysis case, the model explicitly derives potential risks from visual symptoms (e.g., 'loose wiring'), demonstrating strong interpretability. For localization, the `<think>` block explicitly identifies spatial cues (e.g., 'left side') prior to predicting coordinates. This indicates that the model learns to align visual features with spatial positions, ensuring the outputs are supported by image content.

6 Conclusion

UniPCB is a large-scale, bilingual benchmark unifying BPCB and PCBA levels. Structured into three progressive scenarios with 23k QA pairs, it evaluates robustness under varying information density. We propose PCB-GPT, a specialized assistant trained via a three-stage curriculum spanning concept alignment, instruction tuning, and reinforcement learning. This progressive paradigm bridges the domain gap, en-

dowing the model with fine-grained localization and interpretable reasoning absent in general-purpose MLLMs. Future work will focus on scaling UniPCB with production data to advance industrial intelligence.

References

[Anitha and Rao, 2017] DB Anitha and Mahesh Rao. A survey on defect detection in bare pcb and assembled pcb using image processing techniques. In *2017 International conference on wireless communications, signal processing and networking (WiSPNET)*, pages 39–43. IEEE, 2017.

[Bai *et al.*, 2025] Shuai Bai, Keqin Chen, Xuejing Liu, Jialin Wang, Wenbin Ge, Sibo Song, Kai Dang, Peng Wang, Shijie Wang, Jun Tang, et al. Qwen2. 5-vl technical report. *arXiv preprint arXiv:2502.13923*, 2025.

[Chao *et al.*, 2025] Yuhao Chao, Jie Liu, Jie Tang, and Gangshan Wu. Anomalyrl: A grpo-based end-to-end mllm for industrial anomaly detection. *arXiv preprint arXiv:2504.11914*, 2025.

[Chen *et al.*, 2023] Xing Chen, Yonglei Wu, Xingyou He, and Wuyi Ming. A comprehensive review of deep learning-based pcb defect detection. *IEEE Access*, 11:139017–139038, 2023.

[Comanici *et al.*, 2025] Gheorghe Comanici, Eric Bieber, Mike Schaeckermann, Ice Pasupat, Noveen Sachdeva, Inderjit Dhillon, Marcel Blistein, Ori Ram, Dan Zhang, Evan Rosen, et al. Gemini 2.5: Pushing the frontier with advanced reasoning, multimodality, long context, and next generation agentic capabilities. *arXiv preprint arXiv:2507.06261*, 2025.

[Deng *et al.*, 2025] Huilin Deng, Hongchen Luo, Wei Zhai, Yanming Guo, Yang Cao, and Yu Kang. Vmad: Visual-enhanced multimodal large language model for zero-shot anomaly detection. *IEEE Transactions on Automation Science and Engineering*, pages 1–1, 2025.

[Fonseca *et al.*, 2024] Luis Augusto Libório Oliveira Fonseca, Yuzo Iano, Gabriel Gomes de Oliveira, Gabriel Caumo Vaz, Giuliano Paes Carnielli, Júlio César Pereira, and Rangel Arthur. Automatic printed circuit board inspection: a comprehensible survey. *Discover Artificial Intelligence*, 4(1):10, 2024.

[Gu *et al.*, 2024] Zhaopeng Gu, Bingke Zhu, Guibo Zhu, Yingying Chen, Ming Tang, and Jinqiao Wang. Anomalygpt: Detecting industrial anomalies using large vision-language models. In *Proceedings of the AAAI conference on artificial intelligence*, volume 38, pages 1932–1940, 2024.

[Hu *et al.*, 2022] Edward J Hu, Yelong Shen, Phillip Wallis, Zeyuan Allen-Zhu, Yuanzhi Li, Shean Wang, Lu Wang, Weizhu Chen, et al. Lora: Low-rank adaptation of large language models. *ICLR*, 1(2):3, 2022.

[Jiang *et al.*, 2024a] Xi Jiang, Jian Li, Hanqiu Deng, Yong Liu, Bin-Bin Gao, Yifeng Zhou, Jialin Li, Chengjie Wang, and Feng Zheng. Mmad: The first-ever comprehensive benchmark for multimodal large language models in industrial anomaly detection. *arXiv e-prints*, pages arXiv-2410, 2024.

[Jiang *et al.*, 2024b] Yuqi Jiang, Xudong Lu, Qian Jin, Qi Sun, Hanming Wu, and Cheng Zhuo. Fabgpt: An efficient large multimodal model for complex wafer defect knowledge queries. In *Proceedings of the 43rd IEEE/ACM International Conference on Computer-Aided Design*, pages 1–8, 2024.

[Koblah *et al.*, 2023] David Selasi Koblah, Olivia P Dizon-Paradis, Justin Schubeck, Ulbert J Botero, Damon L Woodard, and Domenic Forte. A comprehensive taxonomy of visual printed circuit board defects. *Journal of Hardware and Systems Security*, 7(2):25–43, 2023.

[Kwon *et al.*, 2023] Woosuk Kwon, Zhuohan Li, Siyuan Zhuang, Ying Sheng, Lianmin Zheng, Cody Hao Yu, Joseph Gonzalez, Hao Zhang, and Ion Stoica. Efficient memory management for large language model serving with pagedattention. In *Proceedings of the 29th symposium on operating systems principles*, pages 611–626, 2023.

[Li *et al.*, 2022] Junnan Li, Dongxu Li, Caiming Xiong, and Steven Hoi. Blip: Bootstrapping language-image pre-training for unified vision-language understanding and generation. In *International conference on machine learning*, pages 12888–12900. PMLR, 2022.

[Li *et al.*, 2023] Yuanze Li, Haolin Wang, Shihao Yuan, Ming Liu, Debin Zhao, Yiwen Guo, Chen Xu, Guangming Shi, and Wangmeng Zuo. Myriad: Large multimodal model by applying vision experts for industrial anomaly detection. *arXiv preprint arXiv:2310.19070*, 2023.

[Li *et al.*, 2024a] Bo Li, Yuanhan Zhang, Dong Guo, Renrui Zhang, Feng Li, Hao Zhang, Kaichen Zhang, Peiyuan Zhang, Yanwei Li, Ziwei Liu, et al. Llava-onevision: Easy visual task transfer. *arXiv preprint arXiv:2408.03326*, 2024.

[Li *et al.*, 2024b] Feng Li, Renrui Zhang, Hao Zhang, Yuanhan Zhang, Bo Li, Wei Li, Zejun Ma, and Chunyuan Li. Llava-next-interleave: Tackling multi-image, video, and 3d in large multimodal models. *arXiv preprint arXiv:2407.07895*, 2024.

[Li *et al.*, 2025] Yuanze Li, Shihao Yuan, Haolin Wang, Qizhang Li, Ming Liu, Chen Xu, Guangming Shi, and Wangmeng Zuo. Triad: Empowering lmm-based anomaly detection with vision expert-guided visual tokenizer and manufacturing process, 2025.

[Ling and Isa, 2023] Qin Ling and Nor Ashidi Mat Isa. Printed circuit board defect detection methods based on image processing, machine learning and deep learning: A survey. *IEEE access*, 11:15921–15944, 2023.

[Liu *et al.*, 2023] Haotian Liu, Chunyuan Li, Qingyang Wu, and Yong Jae Lee. Visual instruction tuning. *Advances in neural information processing systems*, 36:34892–34916, 2023.

[Minderer *et al.*, 2022] Matthias Minderer, Alexey Gritsenko, Austin Stone, Maxim Neumann, Dirk Weissenborn, Alexey Dosovitskiy, Aravindh Mahendran, Anurag Arnab, Mostafa Dehghani, Zhuoran Shen, et al. Simple open-vocabulary object detection. In *European conference on computer vision*, pages 728–755. Springer, 2022.

[Ouyang *et al.*, 2022] Long Ouyang, Jeffrey Wu, Xu Jiang, Diogo Almeida, Carroll Wainwright, Pamela Mishkin, Chong Zhang, Sandhini Agarwal, Katarina Slama, Alex Ray, et al. Training language models to follow instructions with human feedback. *Advances in neural information processing systems*, 35:27730–27744, 2022.

[Park *et al.*, 2023] Joon-Hyung Park, Yeong-Seok Kim, Hwi Seo, and Yeong-Jun Cho. Analysis of training deep learning models for pcb defect detection. *Sensors*, 23(5):2766, 2023.

[Peng *et al.*, 2023] Zhiliang Peng, Wenhui Wang, Li Dong, Yaru Hao, Shaohan Huang, Shuming Ma, and Furu Wei. Kosmos-2: Grounding multimodal large language models to the world. *arXiv preprint arXiv:2306.14824*, 2023.

[Radford *et al.*, 2021] Alec Radford, Jong Wook Kim, Chris Hallacy, Aditya Ramesh, Gabriel Goh, Sandhini Agarwal, Girish Sastry, Amanda Askell, Pamela Mishkin, Jack Clark, et al. Learning transferable visual models from natural language supervision. In *International conference on machine learning*, pages 8748–8763. PMLR, 2021.

[Reimers and Gurevych, 2019] Nils Reimers and Iryna Gurevych. Sentence-bert: Sentence embeddings using siamese bert-networks. *arXiv preprint arXiv:1908.10084*, 2019.

[Sankar *et al.*, 2022] V Udaya Sankar, Gayathri Lakshmi, and Y Siva Sankar. A review of various defects in pcb. *Journal of Electronic Testing*, 38(5):481–491, 2022.

[Shao *et al.*, 2024] Zhihong Shao, Peiyi Wang, Qihao Zhu, Runxin Xu, Junxiao Song, Xiao Bi, Haowei Zhang, Mingchuan Zhang, Y. K. Li, Y. Wu, and Daya Guo. Deepseekmath: Pushing the limits of mathematical reasoning in open language models, 2024.

[Sheng *et al.*, 2025] Guangming Sheng, Chi Zhang, Zilingfeng Ye, Xibin Wu, Wang Zhang, Ru Zhang, Yanghua Peng, Haibin Lin, and Chuan Wu. Hybridflow: A flexible and efficient rlhf framework. In *Proceedings of the Twentieth European Conference on Computer Systems*, pages 1279–1297, 2025.

[Tang *et al.*, 2019] Sanli Tang, Fan He, Xiaolin Huang, and Jie Yang. Online pcb defect detector on a new pcb defect dataset. *arXiv preprint arXiv:1902.06197*, 2019.

[Wang *et al.*, 2024] Peng Wang, Shuai Bai, Sinan Tan, Shijie Wang, Zhihao Fan, Jinze Bai, Keqin Chen, Xuejing Liu, Jialin Wang, Wenbin Ge, et al. Qwen2-vl: Enhancing vision-language model’s perception of the world at any resolution. *arXiv preprint arXiv:2409.12191*, 2024.

[Wang *et al.*, 2025] Weiyun Wang, Zhangwei Gao, Lixin Gu, Hengjun Pu, Long Cui, Xingguang Wei, Zhaoyang Liu, Linglin Jing, Shenglong Ye, Jie Shao, et al. Internvl3. 5: Advancing open-source multimodal models in versatility, reasoning, and efficiency. *arXiv preprint arXiv:2508.18265*, 2025.

[Yang *et al.*, 2025] An Yang, Anfeng Li, Baosong Yang, Beichen Zhang, Binyuan Hui, Bo Zheng, Bowen Yu, Chang Gao, Chengan Huang, Chenxu Lv, et al. Qwen3 technical report. *arXiv preprint arXiv:2505.09388*, 2025.

[Yao *et al.*, 2024] Hang Yao, Ming Liu, Haolin Wang, Zhicun Yin, Zifei Yan, Xiaopeng Hong, and Wangmeng Zuo. Glad: Towards better reconstruction with global and local adaptive diffusion models for unsupervised anomaly detection. *arXiv preprint*, 2024.

[Yin *et al.*, 2024] Shukang Yin, Chaoyou Fu, Sirui Zhao, Ke Li, Xing Sun, Tong Xu, and Enhong Chen. A survey on multimodal large language models. *National Science Review*, 11(12):nwae403, 2024.

[Yu *et al.*, 2025a] Ruiyun Yu, Bingyang Guo, and Haoyuan Li. Anomaly detection of integrated circuits package substrates using the large vision model saic: Dataset construction, methodology, and application. In *Proceedings of the IEEE/CVF International Conference on Computer Vision*, pages 22563–22574, 2025.

[Yu *et al.*, 2025b] Tianyu Yu, Zefan Wang, Chongyi Wang, Fuwei Huang, Wenshuo Ma, Zhihui He, Tianchi Cai, Weize Chen, Yuxiang Huang, Yuanqian Zhao, et al. Minicpm-v 4.5: Cooking efficient mllms via architecture, data, and training recipe. *arXiv preprint arXiv:2509.18154*, 2025.

[Zeng *et al.*, 2025] Peijian Zeng, Feiyan Pang, Zhanbo Wang, and Aimin Yang. Lr-iad:mask-free industrial anomaly detection with logical reasoning, 2025.

[Zhang *et al.*, 2019] Tianyi Zhang, Varsha Kishore, Felix Wu, Kilian Q Weinberger, and Yoav Artzi. Bertscore: Evaluating text generation with bert. *arXiv preprint arXiv:1904.09675*, 2019.

[Zhang *et al.*, 2023] Shengyu Zhang, Linfeng Dong, Xiaoya Li, Sen Zhang, Xiaofei Sun, Shuhe Wang, Jiwei Li, Runyi Hu, Tianwei Zhang, Guoyin Wang, et al. Instruction tuning for large language models: A survey. *ACM Computing Surveys*, 2023.

[Zhang *et al.*, 2025] Zongyun Zhang, Jiacheng Ruan, Xian Gao, Ting Liu, and Yuzhuo Fu. Eiad: Explainable industrial anomaly detection via multi-modal large language models. *arXiv preprint arXiv:2503.14162*, 2025.

[Zhao *et al.*, 2025a] Shifang Zhao, Yiheng Lin, Lu Han, Yao Zhao, and Yunchao Wei. Omnid: Detect and understand industrial anomaly via multimodal reasoning, 2025.

[Zhao *et al.*, 2025b] Yuze Zhao, Jintao Huang, Jinghan Hu, Xingjun Wang, Yunlin Mao, Daoze Zhang, Zeyinzi Jiang, Zhikai Wu, Baole Ai, Ang Wang, et al. Swift: a scalable lightweight infrastructure for fine-tuning. In *Proceedings of the AAAI Conference on Artificial Intelligence*, volume 39, pages 29733–29735, 2025.

[Zhou *et al.*, 2023] Yongbing Zhou, Minghao Yuan, Jian Zhang, Guofu Ding, and Shengfeng Qin. Review of vision-based defect detection research and its perspectives for printed circuit board. *Journal of Manufacturing Systems*, 70:557–578, 2023.

[Zhu *et al.*, 2025] Jinguo Zhu, Weiyun Wang, Zhe Chen, Zhaoyang Liu, Shenglong Ye, Lixin Gu, Hao Tian, Yuchen Duan, Weijie Su, Jie Shao, et al. Internvl3: Exploring advanced training and test-time recipes for open-source multimodal models. *arXiv preprint arXiv:2504.10479*, 2025.

UniPCB: A Unified Vision-Language Benchmark for Open-Ended PCB Quality Inspection

Appendix

A Data Curation and Splits

A.1 Data sources and coverage

To maximize the diversity and representativeness of UniPCB, we first conducted a broad survey of PCB quality-inspection datasets spanning both academic benchmarks and industrial collections. This survey serves two purposes: (i) to systematically cover variations in *manufacturing stages* (bare boards vs. assembled boards), *imaging modalities* (optical to X-ray), and *inspection targets* (defects vs. components); and (ii) to provide a comprehensive reference for understanding the current data landscape, including common gaps in accessibility, annotation granularity, and label consistency.

Table 1 summarizes the resulting catalog of *raw candidate datasets* identified during this preliminary phase. Importantly, the table intentionally includes datasets with different accessibility statuses (e.g., private or closed-source industrial datasets). While such datasets are not used to construct the released benchmark, listing them helps contextualize the breadth of real-world inspection data and clarifies which parts of the landscape remain difficult to reproduce publicly.

Field conventions in Table 1. Each source is described using the following attributes:

- **PCB:** Manufacturing stage of the board. *BPCB* denotes bare printed circuit boards (unpopulated), whereas *PCBA* denotes assembled boards populated with electronic components.
- **Mod.:** Imaging modality / acquisition method. We use *RGB* for standard optical images, *AOI* for automated optical inspection systems, *Line-Scan* for linear scanning setups, *Ultrasonic* for ultrasonic imaging, and *AXI* for automated X-ray inspection. When a dataset is collected from in-the-wild or unconstrained environments (as opposed to controlled AOI/AXI pipelines), we denote it as *Real* to emphasize the capture condition and domain shift.
- **Target:** Primary inspection focus. *Defect* indicates anomaly/defect-centric inspection; *Component* focuses on component presence, type, or placement; and *Mix* contains both defects and components.
- **Statistics (#Lab. & #Img.):** **#Lab.** reports the number of categories *after mapping* the original labels to our unified taxonomy, and **#Img.** reports the original number of

images provided by the source.

- **Link:** Public URL or repository entry point for accessing the dataset when available.

Reproducibility note Although Table 1 includes private and closed-source datasets to reflect the full scope of PCB inspection data, the UniPCB benchmark is constructed strictly from the high-quality *open-source* subset. This design choice ensures that UniPCB can be independently reproduced, audited, and extended by the community.

A.2 Preprocessing and Deduplication

Annotation normalization

Given the heterogeneity of source data, we harmonize diverse annotation formats—ranging from segmentation masks to normalized relative coordinates—into a unified axis-aligned bounding box representation. For sources with segmentation masks, we binarize the input and compute the tightest enclosing box derived from the min/max variance of foreground pixels. For annotations provided in relative formats, we project them into absolute pixel space, enforcing rigorous sanitization to clip boundaries, prune degenerate instances, and ensure spatial ordering ($x_1 < x_2, y_1 < y_2$). We adopt absolute pixel coordinates as the exclusive standard to mitigate ambiguity and guarantee compatibility across diverse model architectures (e.g., Qwen2.5 [Bai *et al.*, 2025], which is engineered for absolute inputs).

Global deduplication

To prevent data leakage arising from overlapping tiling, multi-pass captures, or partial re-releases, we execute a global deduplication protocol before any dataset splitting. The pipeline employs a two-level strategy: first removing byte-identical instances via file hashing, followed by perceptual hashing (pHash) to identify near-duplicates caused by minor resizing or compression artifacts. When a duplicate group is detected, we enforce a strict retention hierarchy that prioritizes evaluation integrity: Benchmark > Training. This ensures that visually identical regions—whether full images or overlapping crops—never cross-contaminate the training and evaluation sets.

A.3 Train–Benchmark Isolation

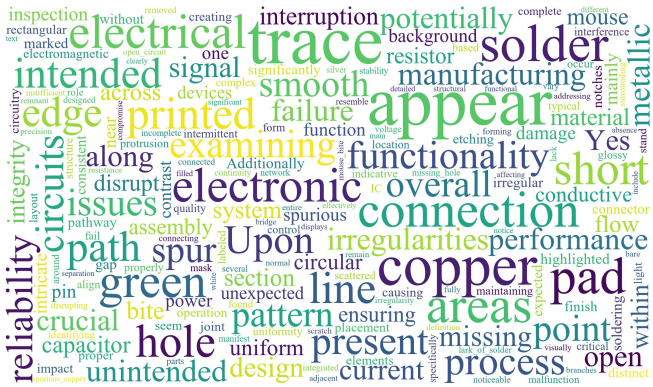
UniPCB is designed to benchmark generalization under realistic inspection constraints. We therefore enforce strict iso-

Dataset	PCB	Mod.	Target	#Lab.	#Img.	Link
HRIPCB [Huang <i>et al.</i> , 2020]	BPCB	RGB	Defect	6	1386	pkusz.edu.cn/
HRIPCB-Augmented [Ding <i>et al.</i> , 2019]	BPCB	RGB	Defect	6	10668	github.com/
DeepPCB [Tang <i>et al.</i> , 2019]	BPCB	Line-Scan	Defect	6	3000	github.com/
PCB-AoI	PCBA	AOI	Defect	1	1211	kaggle.com/
PCBA-DET [Shen <i>et al.</i> , 2024]	PCBA	Real	Defect	8	4601	github.com/
Solder Joint Dataset [Ulger <i>et al.</i> , 2023]	PCBA	Real	Defect	5	3390	github.com/
Dataset-PCB [Ramirez-Farfan and Quiroz-Martinez, 2021]	PCBA	Real	Defect	2	3196	github.com/
DsPCBSD+ [Lei <i>et al.</i> , 2022]	BPCB	AOI	Defect	9	10259	github.com/
PCB-Defect-Detection-Image-Registration [Tanthirige, 2022]	BPCB	Line-Scan	Defect	6	20	github.com/
Defects Dataset	PCBA	Real	Defect	5	484	roboflow.com/
PCB-Defect-Detection	PCBA	RGB	Defect	6	898	roboflow.com/
Mono_PCB Dataset	PCBA	RGB	Defect	16	248	roboflow.com/
Mixed PCB defect [Ancha <i>et al.</i> , 2024]	BPCB	RGB	Defect	6	1741	mendeley.com/
Bangla_PCB_yolo	BPCB	RGB	Defect	6	1196	kaggle.com/
MRC-DETR [Cao <i>et al.</i> , 2025]	BPCB	AOI	Defect	3	800	github.com/
U-PCBD [Lou <i>et al.</i> , 2023]	BPCB	Ultrasonic	Defect	5	4320	iiplab.net/
FICS [Lu <i>et al.</i> , 2020]	PCBA	RGB	Mix	31	9912	trust-hub.org/
VisA (PCB) [Zou <i>et al.</i> , 2022]	PCBA	RGB	Mix	10	4416	github.com/
PCB-Bank [Yao <i>et al.</i> , 2024]	PCBA	RGB	Mix	11	2333	github.com/
PCB-Resistor-Defect-Dataset [Lv <i>et al.</i> , 2024]	PCBA	RGB	Mix	11	261399	github.com/
PCB_Datasets-main	PCBA	AOI	Mix	8	4748	github.com/
PCB AD	PCBA	RGB	Mix	5	690	kaggle.com/
Multiple Datasets on PCB Defects	BPCB	AOI	Mix	2	18493	kaggle.com/
MPI-PCB [Candido de Oliveira <i>et al.</i> , 2023]	PCBA	Real	Mix	2	1797	github.com/
Micro-PCB Images	PCBA	RGB	Component	13	8125	kaggle.com/
FPIC [Jessurun <i>et al.</i> , 2023]	PCBA	AOI	Component	25	6260	ece.ufl.edu/
PCB oriented detection	PCBA	AoI	Component	41	190	kaggle.com/
PCB Component Detection	PCBA	Real	Component	9	1410	ninja.com/
PCB-Components-1495	PCBA	Real	Component	28	830	kaggle.com/
PCB-Component-Detection-CVM	BPCB	RGB	Component	9	101	roboflow.com/
DSLR [Pramerdorfer and Kampel, 2015]	PCBA	RGB	Component	4	748	tuwien.ac.at/
PCB-Vision [Arbash <i>et al.</i> , 2024]	PCBA	RGB	Component	4	106	github.com/
Lite-On Dataset [Chen <i>et al.</i> , 2023]	PCBA	AOI	Mix	8	12200	Private
AXI_PCB_defect_detection [Zhang <i>et al.</i> , 2020]	PCBA	AXI	Mix	4	32377	Private
PCB-METAL [Mahalingam <i>et al.</i> , 2019]	PCBA	RGB	Component	4	984	Private
PCBMO [Li <i>et al.</i> , 2025]	PCBA	RGB	Component	4	3773	Private
PCBSDD [Liao <i>et al.</i> , 2021]	PCB	RGB	Component	6	19029	Private

Table 1: Comprehensive catalog of raw PCB datasets surveyed for the construction of UniPCB. This inventory encompasses diverse PCB types (Bare/Assembled), imaging modalities (RGB, AOI, Line-Scan, X-ray, etc.), and accessibility statuses (Open-source vs. Private). Note that UniPCB selectively curates and standardizes high-quality samples from the open-source subset of these collections.

Stage	Data Composition	Amount
Concept Alignment	1. General image captions: Pixmo [Deitke <i>et al.</i> , 2025] 2. Defect image captions: Defects Dataset, PCB-Defect-Detection, DsPCBSD+, PCBA-en, PCBAD, PCB-Bank, PCB-Resistor-Defect-Dataset-A 3. Component image captions: PCB-Components-1495-A, Micro-PCB Images	~100K
Instruction Tuning	1. General multimodal: LLaVA-1.5 Instruction [Liu <i>et al.</i> , 2023] 2. Defect image multimodal: Bangla_PCB_yolo, Mono_PCB dataset, MRC-DETR, HRIPCB, Mixed PCB defect, HRIPCB-Augmented, PCB_Datasets-main, Multiple Datasets on PCB Defects 3. Component image multimodal: PCB oriented detection, PCB-Components-1495-B	~300K
Reinforcement Learning	1. Defect images: Bangla_PCB, Mono_PCB, MRC-DETR, HRIPCB-Augmented 2. Component images: PCB-Component-Detection-CVM, PCB-Components-1495-B	~5K
Benchmark	1. Defect images: PCBA-DET, Dataset-PCB, PCB-AoI, DeepPCB, VisA(PCB), Solder Joint Dataset, PCB-Defect-Detection-Image-Registration 2. Component images: PCB-Resistor-Defect-Dataset-B, FPIC, PCB-component-detection	~23K

Table 2: Stages, corresponding training datasets, and dataset amounts (some dataset names are abbreviated).



(a) English Subset



(b) Chinese Subset

Figure 1: Bilingual word clouds of the training dataset: (a) English and (b) Chinese high-frequency keywords. Dominant component and defect terms verify the corpus's domain specificity.

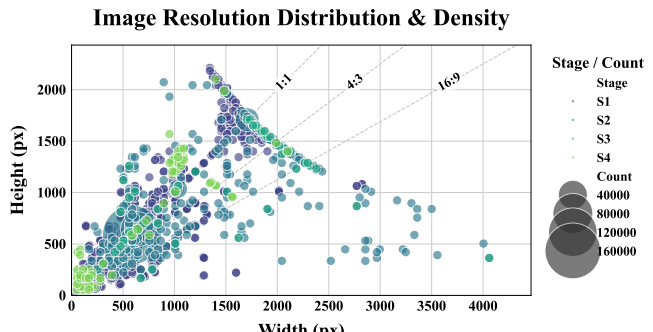


Figure 2: Distribution of image resolutions.

lation between (i) training data used for model development (including curriculum stages) and (ii) the UniPCB benchmark used for reporting results.

Stage-wise curriculum data construction

Table 2 summarizes the four data blocks used in our pipeline: concept-alignment data, instruction-tuning data, reinforce-

ment learning (verifiable) data, and the benchmark set. We use dataset-level partitions whenever possible; for large sources, we create mutually exclusive partitions denoted by suffixes such as “-A” and “-B” and allocate them to different stages to avoid cross-stage contamination.

Isolation strategies

We apply three complementary strategies: (i) Source isolation: benchmark images are preferentially drawn from held-out datasets and held-out partitions. (ii) Cross-split deduplication: we run near-duplicate matching across all splits and remove any overlapping samples. (iii) Rule-level isolation: benchmark prompts/templates are designed independently from training templates to reduce the chance of memorizing surface forms.

A.4 Dataset statistics

To provide a comprehensive characterization of the dataset, Fig. 1 first visualizes the high-frequency keywords in the bilingual subsets, where the prominence of component terms (e.g., “resistor”, “capacitor”) and defect terms (e.g., “short circuit”) confirms that the training corpus contains rich domain-

Category	ID	Name	Description	Impact / Function
Structural	1	Bad Alignment	Misregistration shifts traces or pads.	Opens, shorts, or impedance mismatch.
	2	Hole Offset	Drill hole misaligned relative to pad.	Affects connectivity, insertion; risks opens.
	3	Crack	Substrate or component stress cracks.	Propagates to opens; undermines reliability.
	4	Physical Damage	Breakage or chipping from handling.	Compromises integrity; opens or shorts.
	5	Missing Hole	Required hole undrilled; process failure.	Electrical opens or insertion failure.
	6	Missing Pad	Pad missing; etching or adhesion error.	Prevents attachment; leads to opens.
	7	Mouse Bite	Semi-circular depressions along trace edge.	Reduced current capacity; risk of opens.
Soldering	8	Cold Solder	Dull, grainy surface; insufficient heat.	High resistance; intermittent electrical contact.
	9	Excessive Solder	Convex, bulbous joint exceeds pad.	Risks shorts; masks wetting issues.
	10	Lack of Solder	Low solder volume; insufficient fillet.	Weak joint; intermittent or open circuits.
	11	Pad Corrosion	Oxidized surface from poor storage.	Dewetting; bad contact or opens.
	12	Solder Bridge	Unintended connection between adjacent pads.	Short circuits; device burnout risk.
Component-Related	13	Connector_Damage	Cracked housing or bent pins; poor mating.	Interrupts power/signals; unstable communication.
	14	Pin Damage	Component leads bent, broken, or detached.	Causes poor contact, opens; functional failure.
	15	Missing Component	Component absent, not placed, or detached.	Incorrect functionality or complete module failure.
	16	Missing Switch	Switch physically absent from designated pads.	No user input; control logic fails.
	17	Component Shift	Misaligned component offset from pad center.	Unreliable connections, shorts, or instability.
Wiring connection	18	Open Circuit	Discontinuity in trace, pad, or joint.	Interrupts signals; causes malfunction or failure.
	19	Short Circuit	Unintended connection between isolated conductors.	High current; device burnout or failure.
	20	Spur	Copper projection extending from trace edge.	Bridges gaps; risks shorts, signal noise.
	21	Spurious Copper	Isolated copper in unintended areas.	Risks shorts, parasitic coupling, EMC.
Mechanical	22	Scratch	Abrasion on copper, pad, or mask.	Exposes metal; risks opens, interference.
Contamination	23	Burnt	Localized charring or blistering from heat.	Irreversible structural damage; fire safety hazard.
	24	Contamination	Surface residues: flux, oil, fingerprints, or chemicals.	Causes leakage, corrosion, or poor solder wetting.
	25	Glue Contamination	SMT adhesive residue contaminating the solder pads.	Prevents wetting; leads to dry, unstable joints.
	26	Adhesive Bubbling	Uneven dispensing; trapped air bubbles.	Component shifting, tombstoning, adhesion failure.
Foreign-Matter	27	Foreign Material	Dust, metal chips, or debris.	Shorts, corrosion; reduced reliability.
Control-Computing	1	IC	Microchip (SOP/QFP/BGA) for logic or processing.	Core logic; failure disables major functions.
	2	Microcontroller Board	MCU/SoC-based board (Arduino, Raspberry Pi).	Central controller; failure affects overall operation.
Interconnect	3	Connector	Plug/mate interconnect for cables or modules.	Carries power/signals; disconnect causes failure.
	4	Socket	Receptacle for detachable connections.	Eases maintenance; poor contact drops signal.
	5	Terminal Block	Screw/clamp terminal for external wire connection.	Robust wiring; loosening causes opens or resistance.
	6	Jumper/Header	Pin header with configuration shunt.	Sets mode; missing shunt alters state.
	7	Capacitor	Stores energy; filters, couples, or decouples.	Stabilizes power; failure causes noise or resets.
	8	Inductor	Magnetic storage for filtering or power conversion.	EMI filtering; failure hurts efficiency or stability.
Passive	9	Resistor	Limits current, divides voltage, or biases.	Sets operating points; drift alters circuit limits.
	10	Crystal/Oscillator	Quartz/active oscillator generating system clock.	Provides timing; failure stops MCU logic execution.
	11	Transformer	Voltage conversion and isolation.	Power failure; circuit damage.
	12	LED	Light-emitting diode for status indication.	Visual feedback; failure reduces system observability.
Display-Interaction	13	LCD	Display module for complex visual output.	User interface; failure blocks data display.
	14	Switch	Mechanical switch for power or mode control.	User input; failure breaks interaction or logic.
	15	Buzzer	Audio signaling device (piezo or magnetic).	Audible alarm; failure causes loss of warning.
	16	Potentiometer	Variable resistor for manual calibration/adjustment.	Analog input; wear causes noise or drift.
	17	Diode	One-way device for rectification or protection.	Prevents reverse current; failure risks circuit damage.
Active	18	Transistor	Semiconductor device for switching or amplification.	Signal driver; failure disables loads or overheats.
	19	Relay	Electromechanical switch; high-power isolation.	Mechanical failure; switching stops.
Power-Protection	20	Battery	On-board energy source or backup power.	Power supply; failure causes shutdown or data loss.
	21	Fuse	Protection device; melts at excessive current.	Prevents fire; blown fuse cuts circuit power.
	22	Voltage Regulator	Regulates input to stable voltage rails.	Stabilizes voltage; failure causes system crash.

Table 3: Unified taxonomy of PCB defect and component instances. We provide detailed attributes (Category, ID, Name, Description, Impact/Function, etc.) as textual priors. The IDs link directly to the numerical indices in Fig. 4 and Fig. 5.

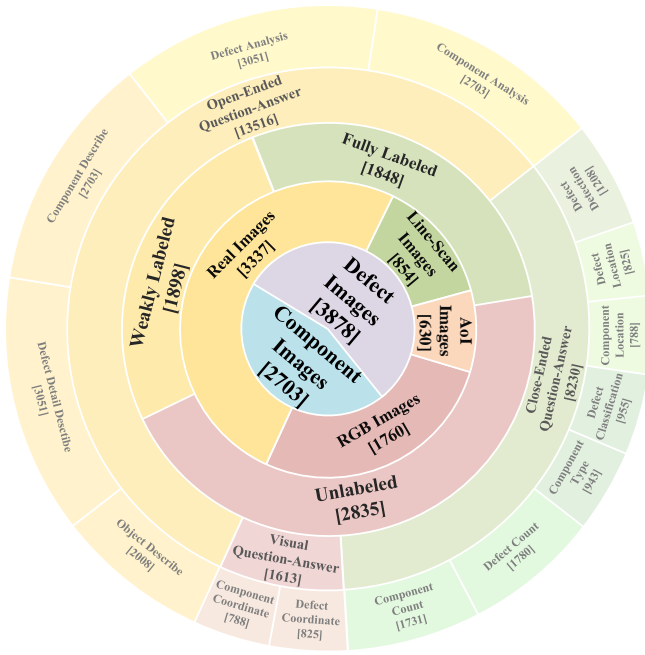


Figure 3: Statistical distribution of the UniPCB Benchmark. The sunburst chart visualizes the hierarchical organization of the benchmark across five nested levels.

specific semantics rather than generic captions. Complementing this textual depth, Fig. 2 illustrates the extensive distribution of image resolutions across Stages 1-4. The dataset spans diverse aspect ratios—from square formats (1:1) to standard photographic (4:3) and wide industrial ratios (16:9)—which prevents the model from overfitting to specific dimensions and necessitates our robust, resolution-agnostic output design. Finally, Fig. 3 details the hierarchical organization of UniPCB Benchmark, flowing from instance counts through diverse modalities (RGB, AOI, Real) and scenarios to specific QA types and 14 distinct inspection subtasks; this design ensures the benchmark jointly varies difficulty while maintaining a unified set of task definitions.

B Unified Taxonomy and Task Schema

B.1 Taxonomy: Definitions and Label Mapping

To establish a consistent and extensible framework, UniPCB consolidates heterogeneous inspection labels into the canonical taxonomy listed in Table 3. Each entry includes a definition, visual symptoms, and functional impact, acting as domain priors for model reasoning. Structurally, we organize the taxonomy hierarchically: defect classes are grouped into high-level families (e.g., structural, soldering, mechanical, contamination) to reflect manufacturing failure modes, while component classes are categorized by functional roles (e.g., control, interconnect, passive, power) to mitigate inter-class similarity in dense layouts. In implementation, we align raw labels from source datasets to these canonical definitions, merging synonymous terms for identical physical failures and discarding samples with underspecified evidence. Fig. 4 and

Fig. 5 visualize the finalized label space, presenting representative exemplars for each category.

B.2 Task Formats and Output Constraints

UniPCB follows practical inspection workflows and defines 14 subtasks spanning detection, counting, classification, localization, description, defect analysis, and re-inspection suggestions. To evaluate robustness under different information density, we provide three scenarios: fully labeled (category and box), weakly labeled (box only), and unlabeled (no annotations).

Answer types

The benchmark incorporates three distinct response formats to evaluate diverse capabilities. Open-ended QA targets high-level description and analysis through free-form generation, whereas Closed-ended QA assesses discrimination ability via multiple-choice or binary questions with fixed answers. Additionally, Visual Grounding demands precise spatial localization, requiring the model to output structured and verifiable coordinates.

Prompts used for generation

Fig. 6 illustrates the progressive prompts used to generate instruction data for our three-stage curriculum: Stage-1 emphasizes observation-centric, caption-like descriptions; Stage-2 introduces task-explicit instructions with deterministic ground-truth alignment for verifiable formats (MCQ and localization); Stage-3 produces omni-task instruction-style conversations with concise user-facing answers and without explicit reasoning tags. Fig. 7 shows the standardized benchmark prompt, which enforces single-answer questions, strict language consistency (English-only or Chinese-only per sample), and type-dependent format constraints (exact-match letters for MCQ and JSON fields for localization) to ensure robust automatic evaluation.

C Quality Control and Supplements

C.1 Dual-track QC and retrospective refinement

To ensure that UniPCB is both reliable and automatically evaluable, we enforce data integrity through a strict dual-track mechanism combining model-based automation with human expertise. The pipeline begins with automated verification, where a lightweight 7B-parameter MLLM is deployed to filter structural anomalies, guaranteeing JSON parsability and basic field completeness before human intervention. Samples clearing this threshold proceed to a hierarchical manual review, where experts validate the data against five logical dimensions: CoT logic consistency, coordinate validity, field completeness, scenario compliance, and JSON formatting. Finally, we establish a retrospective adjustment loop to drive continuous improvement, error patterns identified during manual inspection trigger iterative refinements of the upstream vision prompts and QA rules. Crucially, this mechanism strictly locks the logic of the generated Benchmark Set to ensure evaluation stability, while restricting continuous optimizations to the modifiable training branch.

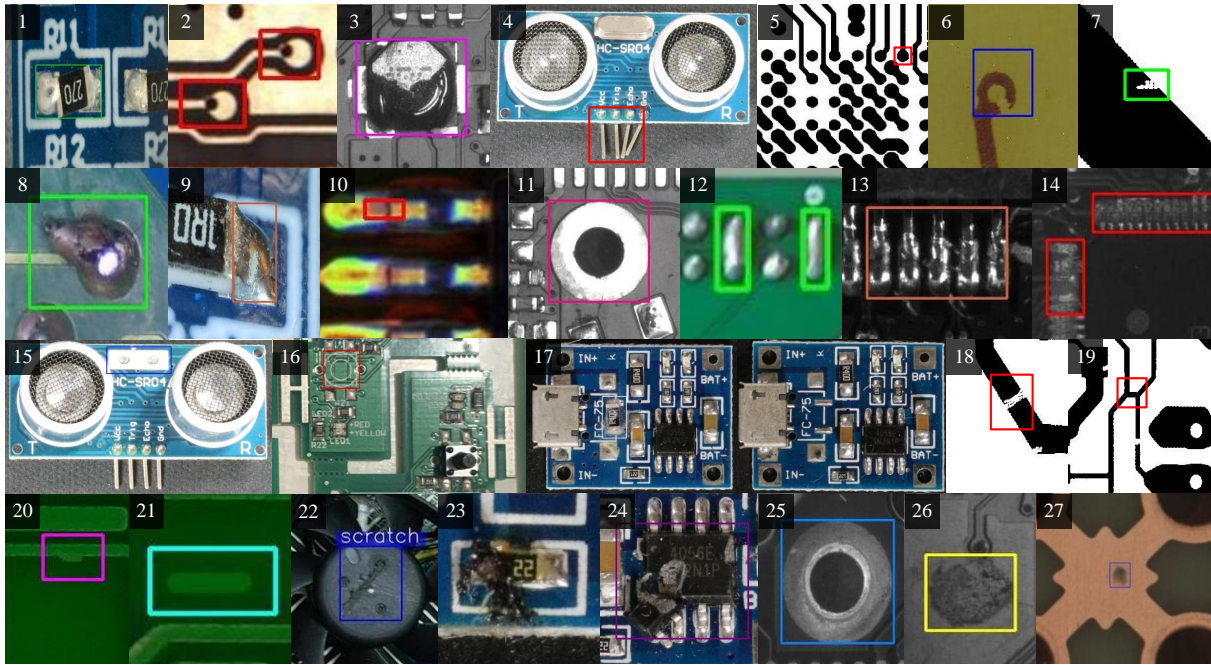


Figure 4: Visual examples of PCB defect instances. The indices in the top-left corners correspond to the IDs in Tab. 3.

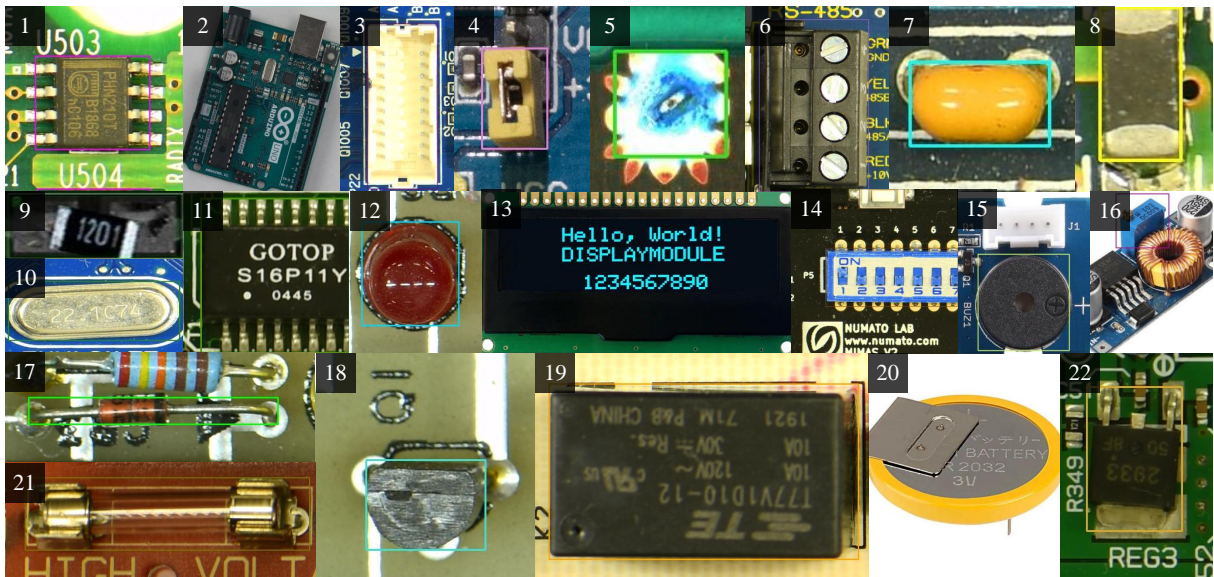


Figure 5: Visual examples of PCB component instances. The indices in the top-left corners correspond to the IDs in Tab. 3.

Stage	LoRA Scope	Rank/ α	Seq Len	LR
Stage1	Attn Q/V	32/64	4096	1e-4
Stage2	All linear	64/128	6144	1e-4
Stage3	All linear	32/64	4096	3e-6

Table 4: Training configurations across the three stages.

C.2 Additional qualitative examples

Fig. 8–10 illustrate the critical performance gap between PCB-GPT and general-purpose baselines across three representative failure modes. In scenarios requiring semantic-spatial alignment, generalist models often exhibit a disconnect between verbal retrieval and visual grounding; for instance, while they may correctly identify a defect like a ‘bent pin’, their predicted bounding boxes frequently drift toward salient background features, indicating a fundamental failure in performing differential analysis. This limitation is exacerbated in crowded PCBA scenes with high inter-class similarity, where baselines exhibit universal failure—often suffering from spatial hallucination by generating boxes on empty traces (e.g., GPT-5), whereas PCB-GPT accurately isolates the target by effectively aligning fine-grained visual cues. Finally, regarding compositional reasoning for co-occurring defects (e.g., ‘lack of solder’ combined with ‘solder bridge’), general models typically display a single-label bias that ignores secondary faults. In contrast, PCB-GPT demonstrates superior reasoning capabilities, aggregating multiple visual evidences to correctly identify compound failure modes rather than defaulting to partial answers.

D Training Configuration

Table 4 summarizes the training configurations across the three curriculum stages, including LoRA scope, rank/ α , sequence length, and learning rate. In Stage-1, we restrict LoRA to attention Q/V projections to preserve general visual ability while injecting PCB semantics. In Stage-2, we apply LoRA to all linear layers to strengthen instruction following and structured generation. In Stage-3, we use a smaller learning rate for stable optimization on verifiable samples.

Prompt for Instruction Data Generation

- Role

You are an AI assistant specialized in PCB inspection, capable of perceiving visual content and providing professional, task-aware responses based on circuit board images.

- Overall Objective

Generate high-quality image–text instruction data for vision–language model training, with progressively stronger supervision on task specificity, reasoning, and instruction following.

Stage-1: Caption-like Visual QA Prompt

- Purpose

To construct natural, observation-driven image–text question answering pairs that resemble human visual inquiries.

- Instructions

1. Generate caption-style questions inspired by the image content.
2. Questions must be natural and descriptive, avoiding task-like instructions.
3. Ground truth knowledge is hidden and may only be used to improve the answer quality.
4. Do not reveal defect types, quantities, locations, or annotations in the question.
5. When multiple QA pairs are generated, each should focus on a different visual aspect.

- Output Format

1. JSON object containing alternating user–assistant turns.
2. Each user turn must start with <image> followed by the question.

Stage-2: Task-oriented Visual Instruction Prompt

- Purpose

To generate task-explicit visual instructions targeting specific inspection capabilities.

- Instructions

1. Each question must correspond to a predefined task type (e.g., detection, count, classification, location, analysis).
2. Questions are task-aware and image-grounded.
3. Explicit reasoning is required for selected tasks to guide visual inference.
4. Deterministic tasks must match the ground truth exactly.
5. Answers must follow the structured format:
<think>Visual evidence and step-by-step reasoning.</think>
<answer>Final task-specific answer.</answer>

- Constraints

1. Ground truth information must not appear in the question.
2. Reasoning must be visually grounded and avoid referencing labels, annotations, or ground truth terms.
3. Deterministic tasks require answers that strictly match the ground truth.

Stage-3: Omni-task Instruction Conversation Prompt

- Purpose

To align the model with real-world instruction-following behavior across diverse visual tasks.

- Instructions

1. Support diverse task formats, including: QA, multiple-choice questions, yes/no questions, and structured outputs.
2. Questions must remain task-aware and image-grounded.
3. Responses should be concise, professional, and user-facing.
4. Do not include explicit reasoning tags (e.g., <think>).
5. Multi-turn conversations may combine multiple tasks over the same image.

- Output

1. Instruction-style conversations suitable for large-scale instruction tuning.
2. Clean answers without exposed internal reasoning.

Figure 6: The progressive prompts used to generate the three-stage curriculum instruction tuning data.

Prompt for Benchmark Construction

- **Role**

You are an AI assistant for constructing standardized PCB inspection benchmarks with unambiguous questions and automatically verifiable answers.

- **Overall Objective**

To generate evaluation-ready VQA and multiple-choice questions with fixed answers, controlled difficulty, and consistent language, enabling reliable model comparison.

- **Instructions**

1. Generate benchmark questions based on image content and dataset annotations.
2. Each question must have a single correct answer.
3. For multiple-choice questions:
 - (1) Generate one correct option and multiple plausible distractors.
 - (2) Distractors must be consistent in style and length while being clearly incorrect.
4. Enforce strict language consistency (Chinese or English only).
5. Output must be machine-readable and suitable for automatic scoring.

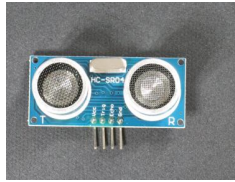
- **Supported Question Types**

1. Object description
2. Defect: detection, classification, count, location, coordinates, analysis
3. Component: type, count, location, description, coordinates, analysis
4. Comparative questions (e.g., OK vs. NG)

- **Output Format**

1. JSON with explicit fields for:
 - (1) question
 - (2) correct_option
 - (3) options (if applicable)
2. Structured coordinate outputs when required.

Figure 7: The standardized prompt used for UniPCB benchmark construction.



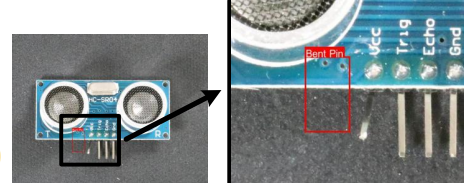
Question:

Comparing the normal and abnormal images, Find the absolute bounding box coordinates for the bent defect(s) in the image.

Inside <answer>, output ONLY JSON coordinates: {"Category Name": [[x1,y1,x2,y2], ...], ...}.

GPT-5:

<answer> { "Bent Pin": [[430, 690, 520, 840]] } </answer>

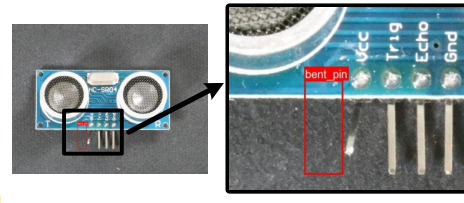


Gemini2.5-Pro:

Based on the visual comparison between the normal and abnormal images, the defect is identified as a bent pin on the ultrasonic sensor module (HC-SR04).

Specifically, the leftmost pin (typically the Vcc pin) is bent significantly to the left compared to the straight alignment seen in the normal reference image.

<answer> { "bent_pin": [[465, 720, 535, 890]] } </answer>

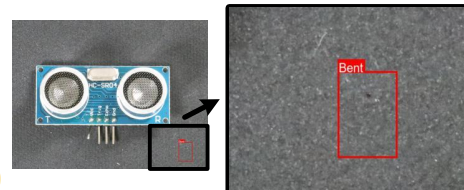


Claude-Sonnet 4.5:

Looking at the two images, I can identify the bent defect by comparing the normal image with the abnormal image.

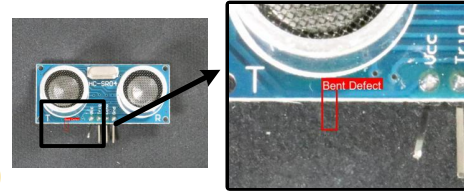
The bent defect is visible on one of the four pin connectors at the bottom of the module. In abnormal image, the rightmost pin appears to be bent compared to normal image where all pins are straight.

<answer> { "Bent": [[0.85, 0.82, 0.92, 0.95]] } </answer>



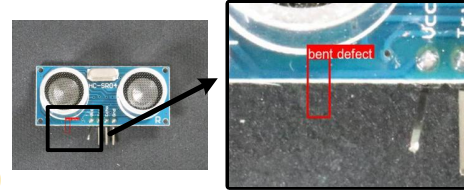
Doubao-seed-v1.6:

{"Bent Defect": [[375,730,403,804]]}



Qwen3-Max:

<answer> { "bent defect": [[380,715,416,804]] } </answer>



PCB-GPT:

<think>In the first image, there is a noticeable deformation on one of the pins at the bottom left corner, which aligns with the definition of a bent defect as it involves a pin that has been bent out of its original position. The second image does not show any such deformation, confirming the presence of a bent defect in the first image.</think>

<answer> { "bent": [[528, 790, 613, 884]] } </answer>

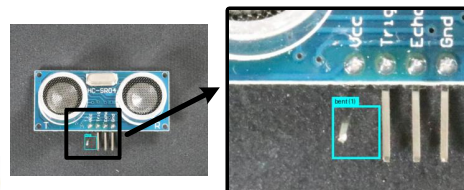


Figure 8: Visualization of reference-based defect localization. The example targets a “bent pin” defect on an ultrasonic sensor, utilizing a normal reference image and a query image. The text panel displays the internal <think> process preceding the final coordinate output.



Question:

Find the bounding box coordinates for the IC in the image.
Think before answering. Your final reply must ONLY contain:

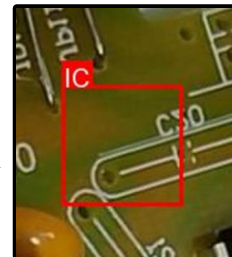
<think>...</think><answer>...</answer>.

Inside <answer>, output ONLY JSON coordinates:
{ "Category Name": [[x1,y1,x2,y2], ...], ... }.

GPT-5:

<think>Locate the small black rectangular chip with dual-side pins and mark its bounding region.</think>

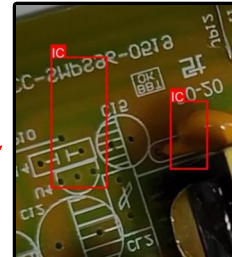
<answer> { "IC": [[515, 410, 610, 505]] } </answer>



Gemini2.5-Pro:

<think>This is a Switching Mode Power Supply (SMPS) PCB. It mainly features a central yellow transformer for voltage conversion, electrolytic capacitors for filtering, and control chips (an 8-pin IC and optocoupler) for regulation.</think>

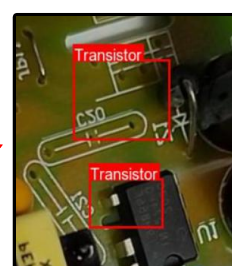
<answer> { "IC": [[605, 371, 715, 466], [626, 516, 708, 585]] } </answer>



Claude-Sonnet 4.5:

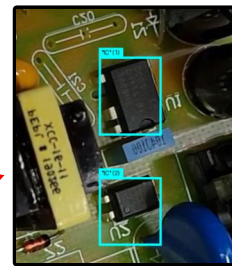
<think>Looking at the PCB image to identify IC components. The image appears to be approximately 800x1200 pixels. Main ICs visible: Black rectangular IC in center-left area - approximately (220, 420) to (310, 630) Smaller black IC/component on right side - approximately (410, 490) to (470, 600)</think>

<answer> { "IC": [[220, 420, 310, 630], [410, 490, 470, 600]] } </answer>



Doubao-seed-v1.6:

{ "Category Name": [[610, 406, 726, 521], [626, 542, 722, 622]] }



PCB-GPT:

<think>Observing the image, there are two rectangular components with multiple pins that appear to be integrated circuits (ICs). These components are located at specific positions on the board and have distinct shapes compared to other elements like capacitors and resistors. The bounding boxes for these ICs can be determined by identifying their edges relative to the overall dimensions of the PCB.</think>

<answer> { "IC": [[635, 504, 742, 639], [635, 711, 742, 828]] } </answer>

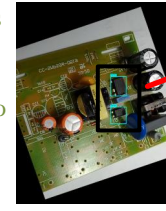
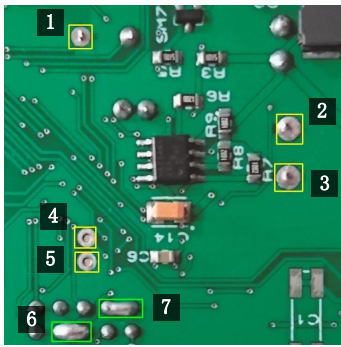


Figure 9: Visualization of dense component localization. The task requires identifying the bounding box of an 'IC' (Integrated Circuit).



Question:

Regarding the labeled target in the image, what is its type?

- A. solder bridge.
- B. component damaged.
- C. lack of solder and open circuit.
- D. lack of solder and solder bridge.

Select the option you think is correct and output only its uppercase letter.

Think before answering. Your final reply must ONLY contain:

<think>...</think><answer>...</answer>

Inside <answer>, output ONLY one letter A/B/C/D.

GT:

<answer>A</answer>.

GPT-5:

<think>The image shows multiple labeled regions: yellow boxes indicate insufficient solder (lack of solder) on through-holes, and green boxes at the bottom indicate solder bridges between pads. Therefore, the labeled targets include both lack of solder and solder bridge defects.</think>



<answer>D</answer>

Gemini2.5-Pro:

<think>The yellow boxes indicate a lack of solder on individual joints, while the green boxes highlight solder bridges connecting multiple pads; therefore, option D correctly identifies both defect types present in the image.</think>



<answer>D</answer>

<think>Looking at this PCB image, several areas are highlighted with yellow boxes. The highlighted spots appear to be solder joints or vias. Examining them closely, particularly the two circular areas on the lower left, they seem to show insufficient solder coverage or missing solder. This type of defect would prevent proper electrical connection, resulting in an open circuit. I don't see evidence of solder bridges (unwanted connections between pads) or damaged components. The defect pattern is consistent with inadequate soldering leading to connectivity issues, making option C the most appropriate answer.</think>



<answer>C</answer>

A



Qwen3-Max:

<answer>C</answer>



Grok:

<think>The labeled targets (green and yellow boxes) point to several solder joints around components like the IC, resistors, and capacitors. Most appear to have insufficient solder fillet or barely any solder coverage on the pads, indicating poor wetting or missing solder material, which can lead to open circuits. There is no clear continuous solder blob connecting adjacent pads that would qualify as a solder bridge. No components show visible cracking, breaking, or obvious physical damage either. Therefore the primary defect visible in the labeled areas is lack of solder (and potential open circuit as a consequence), not bridging or component damage.</think>



<answer>C</answer>

PCB-GPT:

<think>Observing the highlighted areas on the PCB, there are visible signs of soldering issues such as insufficient solder coverage around the pads and pins, which can lead to poor electrical connections. The highlighted regions indicate potential solder bridges where solder has spread beyond intended connections, leading to unintended conductive paths between components that should be isolated.</think>



<answer>D</answer>

Figure 10: Visualization of multi-type defect classification. The task requires identifying co-existing defects ('lack of solder' and 'solder bridge') and selecting the corresponding compound option (D) from the multiple-choice list.

References

[Ancha *et al.*, 2024] Vinod Kumar Ancha, Fadi N Sibai, Venkateswarlu Gonuguntla, and Ramesh Vaddi. Utilizing yolo models for real-world scenarios: Assessing novel mixed defect detection dataset in pcbs. *IEEE Access*, 2024.

[Arbash *et al.*, 2024] Elias Arbash, Margret Fuchs, Behnoor Rasti, Sandra Lorenz, Pedram Ghamisi, and Richard Gloaguen. Pcb-vision: A multiscene rgb-hyperspectral benchmark dataset of printed circuit boards. *IEEE Sensors Journal*, 24(10):17140–17158, 2024.

[Bai *et al.*, 2025] Shuai Bai, Keqin Chen, Xuejing Liu, Jialin Wang, Wenbin Ge, Sibo Song, Kai Dang, Peng Wang, Shijie Wang, Jun Tang, et al. Qwen2. 5-vl technical report. *arXiv preprint arXiv:2502.13923*, 2025.

[Candido de Oliveira *et al.*, 2023] Diulhio Candido de Oliveira, Bogdan Tomoyuki Nassu, and Marco Aurelio Wehrmeister. Image-based detection of modifications in assembled pcbs with deep convolutional autoencoders. *Sensors*, 23(3):1353, 2023.

[Cao *et al.*, 2025] Jiangzhong Cao, Huanqi Wu, Xu Zhang, Lianghong Tan, and Huan Zhang. Mrc-detr: An adaptive multi-residual coupled transformer for bare board pcb defect detection. *arXiv preprint arXiv:2507.03386*, 2025.

[Chen *et al.*, 2023] I-Chun Chen, Rey-Chue Hwang, and Huang-Chu Huang. Pcb defect detection based on deep learning algorithm. *Processes*, 11(3):775, 2023.

[Deitke *et al.*, 2025] Matt Deitke, Christopher Clark, Sangho Lee, Rohun Tripathi, Yue Yang, Jae Sung Park, Mohammadreza Salehi, Niklas Muennighoff, Kyle Lo, Luca Soldaini, et al. Molmo and pixmo: Open weights and open data for state-of-the-art vision-language models. In *Proceedings of the Computer Vision and Pattern Recognition Conference*, pages 91–104, 2025.

[Ding *et al.*, 2019] Runwei Ding, Linhui Dai, Guangpeng Li, and Hong Liu. Tdd-net: a tiny defect detection network for printed circuit boards. *CAAI Transactions on Intelligence Technology*, 4(2):110–116, 2019.

[Huang *et al.*, 2020] Weibo Huang, Peng Wei, Manhua Zhang, and Hong Liu. Hripcb: a challenging dataset for pcb defects detection and classification. *The Journal of Engineering*, 2020(13):303–309, 2020.

[Jessurun *et al.*, 2023] Nathan Jessurun, Olivia P Dizon-Paradis, Jacob Harrison, Shajib Ghosh, Mark M Tehraniipoor, Damon L Woodard, and Navid Asadizanjani. Fpic: a novel semantic dataset for optical pcb assurance. *ACM Journal on Emerging Technologies in Computing Systems*, 19(2):1–21, 2023.

[Lei *et al.*, 2022] Ruoshan Lei, Dongpeng Yan, Hongjin Wu, and Yibing Peng. A precise convolutional neural network-based classification and pose prediction method for pcb component quality control. In *2022 14th International Conference on Electronics, Computers and Artificial Intelligence (ECAI)*, pages 1–6. IEEE, 2022.

[Li *et al.*, 2025] Jingxuan Li, Feipeng Da, and Yi Yu. Pcb-ssd: Self-supervised symmetry-aware detector for pcb displacement and orientation inspection. *Measurement*, 243:116342, 2025.

[Liao *et al.*, 2021] Xinting Liao, Shengping Lv, Denghui Li, Yong Luo, Zichun Zhu, and Cheng Jiang. Yolov4-mn3 for pcb surface defect detection. *Applied Sciences*, 11(24):11701, 2021.

[Liu *et al.*, 2023] Haotian Liu, Chunyuan Li, Qingyang Wu, and Yong Jae Lee. Visual instruction tuning. *Advances in neural information processing systems*, 36:34892–34916, 2023.

[Lou *et al.*, 2023] Liangshan Lou, Ke Lu, and Jian Xue. Multi-scale vision transformer for defect object detection. *Procedia Computer Science*, 222:397–406, 2023.

[Lu *et al.*, 2020] Hangwei Lu, Dhwani Mehta, Olivia Paradis, Navid Asadizanjani, Mark Tehraniipoor, and Damon L Woodard. Fics-pcb: A multi-modal image dataset for automated printed circuit board visual inspection. *Cryptology ePrint Archive*, 2020.

[Lv *et al.*, 2024] Shengping Lv, Bin Ouyang, Zhihua Deng, Tairan Liang, Shixin Jiang, Kaibin Zhang, Jianyu Chen, and Zhuohui Li. A dataset for deep learning based detection of printed circuit board surface defect. *Scientific Data*, 11(1):811, 2024.

[Mahalingam *et al.*, 2019] Gayathri Mahalingam, Kevin Marshall Gay, and Karl Ricanek. Pcb-metal: A pcb image dataset for advanced computer vision machine learning component analysis. In *2019 16th International Conference on Machine Vision Applications (MVA)*, pages 1–5. IEEE, 2019.

[Pramer Dorfer and Kampel, 2015] Christopher Pramer Dorfer and Martin Kampel. A dataset for computer-vision-based pcb analysis. In *2015 14th IAPR international conference on machine vision applications (MVA)*, pages 378–381. IEEE, 2015.

[Ramirez-Farfan and Quiroz-Martinez, 2021] Alberto-Santiago Ramirez-Farfan and Miguel-Angel Quiroz-Martinez. System for troubleshooting welded printed circuit boards with through hole technology using convolutional neural networks and classic computer vision techniques. In *The International Conference on Advances in Emerging Trends and Technologies*, pages 199–208. Springer, 2021.

[Shen *et al.*, 2024] Minghui Shen, Yujie Liu, Jing Chen, Kangqi Ye, Heyuan Gao, Jie Che, Qingyang Wang, Hao He, Jian Liu, Yan Wang, et al. Defect detection of printed circuit board assembly based on yolov5. *Scientific Reports*, 14(1):19287, 2024.

[Tang *et al.*, 2019] Sanli Tang, Fan He, Xiaolin Huang, and Jie Yang. Online pcb defect detector on a new pcb defect dataset. *arXiv preprint arXiv:1902.06197*, 2019.

[Tanthirige, 2022] Nandeera Kamalaja De Silva Munaweera Tanthirige. *Printed Circuit Board Defect Detection Using Image Processing*. Minnesota State University, Mankato, 2022.

[Ulger *et al.*, 2023] Furkan Ulger, Seniha Esen Yuksel, Atila Yilmaz, and Dincer Gokcen. Solder joint inspection on printed circuit boards: A survey and a dataset. *IEEE Transactions on Instrumentation and Measurement*, 72:1–21, 2023.

[Yao *et al.*, 2024] Hang Yao, Ming Liu, Haolin Wang, Zhicun Yin, Zifei Yan, Xiaopeng Hong, and Wangmeng Zuo. Glad: Towards better reconstruction with global and local adaptive diffusion models for unsupervised anomaly detection. *arXiv preprint*, 2024.

[Zhang *et al.*, 2020] Qianru Zhang, Meng Zhang, Chinthaka Gamanayake, Chau Yuen, Zehao Geng, Hirunima Jayasekara, Xuewen Zhang, Chia-wei Woo, Jenny Low, and Xiang Liu. Deep learning based defect detection for solder joints on industrial x-ray circuit board images. *arXiv preprint arXiv:2008.02604*, 2020.

[Zou *et al.*, 2022] Yang Zou, Jongheon Jeong, Latha Pemula, Dongqing Zhang, and Onkar Dabeer. Spot-the-difference self-supervised pre-training for anomaly detection and segmentation. In *European conference on computer vision*, pages 392–408. Springer, 2022.